*fishes*

MDPI

*Article*

# Effects of Different Culture Densities on the Acoustic Characteristics of *Micropterus salmoide* Feeding

**Renyu Qi [1,2], Huang Liu [2,*] and Shijing Liu [2]**

[1] College of Fisheries and Life Science, Shanghai Ocean University, Shanghai 201306, China
[2] Fishery Machinery and Instrument Research Institute, Chinese Academy of Fishery Sciences, Shanghai 200092, China
* Correspondence: liuhuang@fmiri.ac.cn; Tel.: +86-186-0177-1215

**Abstract:** The intensity and frequency of the acoustic signals generated by different behaviors of largemouth bass (*Micropterus salmoides)* have different characteristics. The acoustic signals generated during feeding can be used to analyze the characteristic patterns of their used behavior, which can provide a theoretical basis for applications such as automatic feeding based on acoustic signals. We used passive acoustics combined with video to study the feeding acoustic signals of largemouth bass in a recirculating water culture system (4, 8, 12, and 16 fish/$m^3$). The result of the time–frequency and power spectrum analysis of the feeding sound signals showed that the short-time average amplitude of the feeding signal was well distinguished from the background noise, both the swallowing and the chewing sounds were positively correlated with the culture density, and the correlation between the swallowing sound and number of fish was stronger; at different culture densities, the short-time average zero-crossing in the swallowing phase of the largemouth bass suddenly dropped to about 500 and rose to about 1000 in the chewing process. Therefore, both the chewing and the swallowing sounds can be used as parameters to automatically identify the largemouth bass feeding process signal. The spectrum entropy in the feeding process of the largemouth bass was maintained at about 4–6 for different culture densities. In the power spectrum, the main feeding sounding frequencies of the largemouth bass at different farming densities and the distinguishable spectral range of the background noised ranged from 1 to 20 kHz, the main peak frequency of the feeding sound was within the range of 1.2 to 3.0 kHz, and the main power value of the power spectrum was positively correlated with farming density.

**Keywords:** aquaculture; largemouth bass; feeding behavior; feeding signals

**Key Contribution:** The acoustic characteristics of *Micropterus salmoides* feeding were studied using a passive acoustic technique. The acoustic parameters which can be used for the recognition of feeding sound are analyzed in the time domain and frequency domain.

check for updates

**Citation:** Qi, R.; Liu, H.; Liu, S. Effects of Different Culture Densities on the Acoustic Characteristics of *Micropterus salmoide* Feeding. *Fishes* **2023**, *8*, 126. https://doi.org/10.3390/fishes8030126

Academic Editors: Chi-Fang Chen and Kwang-Tsao Shao

Received: 9 January 2023
Revised: 15 February 2023
Accepted: 21 February 2023
Published: 23 February 2023

**Copyright:** © 2023 by the authors. Licensee MDPI, Basel, Switzerland. This article is an open access article distributed under the terms and conditions of the Creative Commons Attribution (CC BY) license (https://creativecommons.org/licenses/by/4.0/).

## 1. Introduction

Fish behavior can visually reflect the state of feeding, reproduction, stress, and other activities in aquaculture [1,2], and an in-depth study of fish behavior can provide important information and guidance for aquaculture. Vocalization is an important fish behavior, and acoustic signals accompany different activities such as reproduction, territorial behavior, foraging, and swimming [3,4]. Fish have a variety of different vocal mechanisms that can be broadly divided into active and passive vocalizations; for example, fish in the process of breathing exhibit these vocalizations due to the rhythmic movement of the gill covers and breathing sounds [5]; Moreover, some male fish living on the bottom with their bodies or fins touching or hitting the ground create sounds to court female fish [6]. The signal intensity and frequency generated by different fish behaviors are different; hence, analyzing and quantifying the feeding sound signals of fish and determining the feeding

sound characteristics of fish can provide theoretical guidance for the intelligent feeding of aquatic fish [7–9].

Scholars in the field of aquatic animal behavior detection widely use passive acoustic technology as a noninvasive behavior detection method [10–12]. They rely on this technology to analyze aquatic animal feeding behavior and patterns, and in doing so, they reduce feed costs and increase farming efficiency [13]. The sound characteristics of *Litopenaeus vannamei* are similar when feeding on feeds of different particle sizes, with frequencies ranging from 5 to 45 kHz, and their feeding sound signals can be collected both in ponds and in the laboratory [14]. *Penaeus monodon* produce acoustic signals during feeding that can be used to identify feeding activity and determine, on a net and pond basis, if this feeding sound is linearly correlated with feed consumption [15]. The variation in the sound pressure level during feeding of turbot (*Scophthalmus maximus*) feeding is 15–20 dB, and this variation can reflect the variation in the feeding sound intensity and can be used to develop a fish feeding sound detector [16]. Tilapia feeding sounds range from 0 to 6 kHz, and the sound power is positively correlated with the feeding vigor, which can be combined with growth and feeding models to develop appropriate feeding [17].

Many scholars have studied the characteristics of the feeding acoustic signals of largemouth bass (*Micropterus salmoides*). By grouping largemouth bass in experiments, Qu et al. found that the feeding acoustic signals of largemouth bass of different body lengths could be distinguished from background noise in the frequency range of 1–10 kHz, the acoustic signal pulse width mainly centered around 3 ms, and the difference at the first resonance peak was small [18]. Cao et al. [19] showed that the feeding signals of largemouth bass mainly concentrated in the energy range of 4.2–7.4 kHz via acoustic synchronization, the feeding interval and swallowing order were positively correlated, and the resonance peak and Meier's cepstrum coefficient could be used as the identification parameters of the largemouth bass feeding sound. However, neither of these studies considered the fact that the breeding density might affect the feeding sound of largemouth bass. Therefore, we fed pellet feed to an experimental group of largemouth bass at different culture densities in the laboratory to record their feeding acoustic signals. We used a sound acquisition device and a camera to obtain image data to determine the acoustic signal characteristics of largemouth bass at different culture densities. The results of this study can provide theoretical support for applications such as automatic feeding based on feeding vocal signals in aquacultures.

## 2. Material and Methods

### *2.1. Test Subjects*

We selected largemouth bass as the test material for this experiment, and we purchased the fry from Acoman(Shanghai, China) Agriculture Co. We reared the fish in a 1.5 m × 1 m × 1.5 m glass tank with a 1 $m^3$ water volume. Table 1 shows the specific test grouping. The water temperature of the culture environment during the test was 28.6 ± 2.2 °C, the dissolved oxygen level was 5.83 ± 1.69 mg/L, and the pH value was 7.54 ± 1.01. The feeds investigated were special feeds for largemouth bass from Yisheng Aquatic Co. (Hangzhou, China). During the experiment, we fed each group once (9:00 a.m.) and twice (9:00 a.m. and 7:00 p.m.), and the daily feeding amount was no more than 5% of the fish body weight; the weight of the feed was essentially the same for each group.

**Table 1.** Grouping table of test subjects.

| Group | Quantity (Fish) | Body Length (cm) | Body Weight (g) | Breeding Density (Fish·$m^{-3}$) |
|---|---|---|---|---|
| F1 | 4 | 26.25 ± 2.63 | 308.75 ± 26.93 | 4 |
| F2 | 8 | 27.13 ± 2.41 | 310.86 ± 23.21 | 8 |
| F3 | 12 | 27.42 ± 2.97 | 319.25 ± 34.68 | 12 |
| F4 | 16 | 27.00 ± 2.76 | 314.50 ± 31.57 | 16 |

### 2.2. Acoustic Signal and Video Capture

We used a largemouth black bass acoustic signal acquisition system with a filter pool and small circulating water system, hydrophone (model: AQH-020; frequency range: 20 Hz–20 kHz, Kyoto, Japan), preamplifier (model: Aquafeeler IV; gain control: 20–70 dB, Kyoto, Japan), and Roland QUAD-CAPTURE external sound card (model: UA-55, Taiwan Leland Enterprise Co., Ltd., Taiwan, China). The video recording device was a SPORTS CAMERA 4K HD antishake digital video camera (model: QOER V70, Shenzhen True Vision Technology Co., Shenzhen, China). We recorded the largemouth bass feeding process using the method of sound and video synchronization; additionally, we turned the circulating water system was turned off during the sound acquisition, and we recorded the environmental background noise for 5 min before each feeding. The acquisition time was 15 min, the sampling frequency of the recording was 9.6 kHz, the sampling accuracy was 24 bit, the sampling channel was a single channel, and the signal gain was 50 dB. We saved the acquired audio and video onto a computer, and we subsequently processed the audio and video with Matlab 2019a, version 9.6.0.1072779 and Adobe Audition version 13.0.1.35, for signal preprocessing and feature analysis, respectively.

### 2.3. Determination of Feeding Signals

In the sound signal acquisition process, the fish gradually adapted to lying still in the tank after the hydrophone entered the water. After 5 min of signal acquisition, feed was put into the tank (near the hydrophone); it was found that the largemouth bass started to feed within a short time after feeding, and the feeding vocal signal could be detected at this time.

By observing the waveform graph of each group of signals collected, there was almost no vocal signal in the 5 min before baiting. Combined with the videos, it can be determined that largemouth bass started to swim in search of feed and subsequently ingested after baiting. Figure 1 shows the changes in waveform graph, spectrogram, and relative sound pressure comparing before and after feeding. It can be found that the energy during the feeding period of largemouth bass was higher than that during the nonfeeding period, indicating that a certain number of feeding vocal signals were generated during the feeding process, and no other noise interfered with the feeding process. The vocalization signals were selected from the waveform plots that determined the feeding.

### 2.4. Acoustic Signal Preprocessing

The collected acoustic signals contained noise, which would have reduced the experimental data accuracy if directly used. Therefore, we performed preprocessing operations before extracting the characteristics of the largemouth bass acoustic signal. We mainly used the preprocessing method according to Cao et al. [19] to enhance the high-frequency part of the signal using a pre-emphasis digital filter to smooth the spectrum in the whole frequency band from low to high frequency with a pre-emphasis factor of 0.87. After that, we framed and windowed the acoustic signal. The shape and length of the window function were two important parameters for the time domain analysis of the ingestion signal. The Hamming window could eliminate the side flaps, and the main flaps were relatively narrow; hence, the continuity between the beginning and end of the signal frames was stable. Then, a subspace speech enhancement algorithm combined with a high-throughput algorithm was used to noise reduce the ingestion acoustic signal.

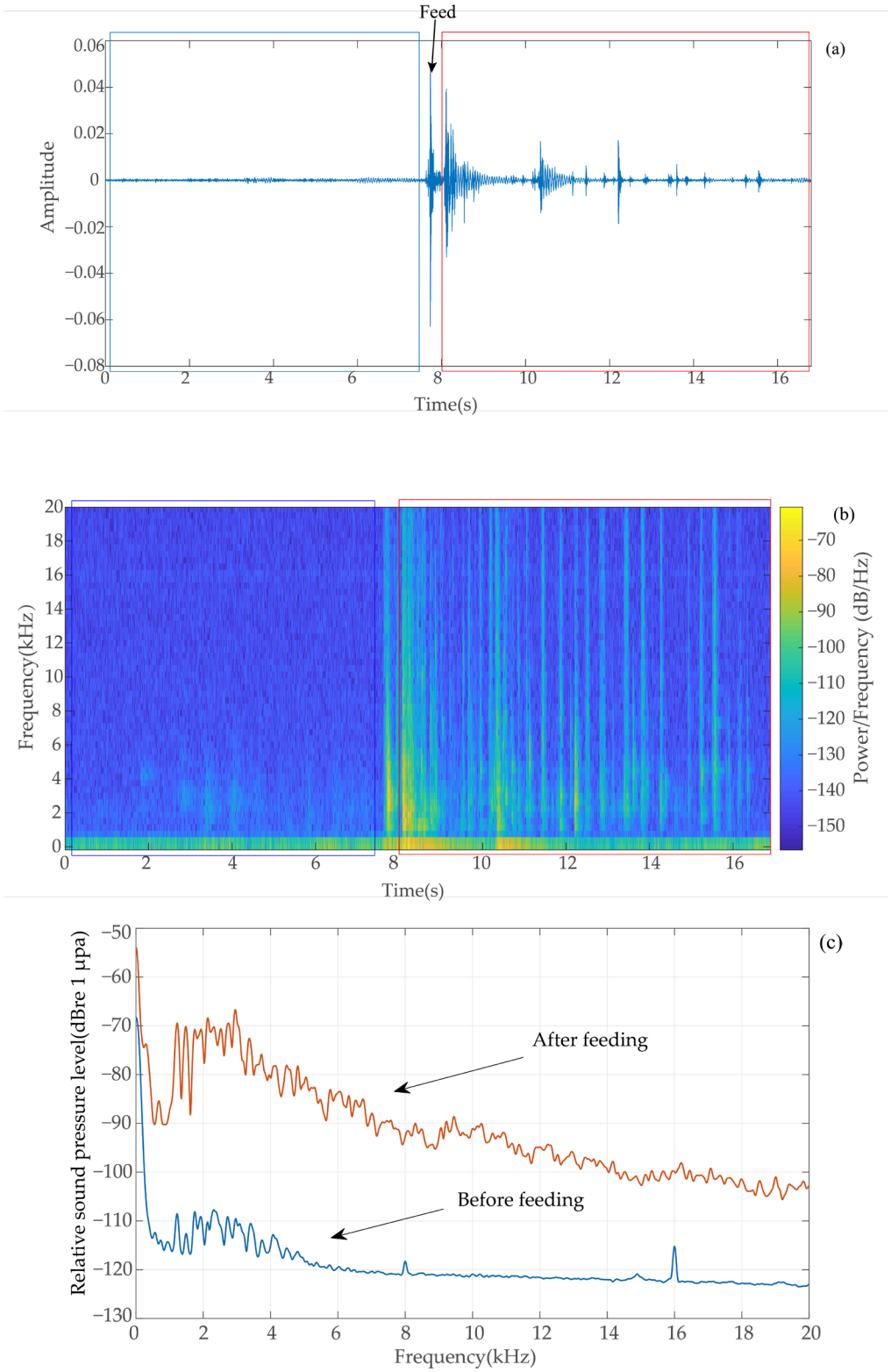



**Figure 1.** Comparison of waveform (**a**), spectrograms (**b**), and relative sound pressure (**c**) before and after feeding (unreduced noise).

### *2.5. Extraction of Ingestion Sound Signal Features*

The acoustic signal itself was a time domain signal, and a complete largemouth bass feeding acoustic signal mainly consisted of two parts: swallowing and chewing sounds. For the complete feeding sound signal, the time-domain features such as the short-time

average amplitude, short-time average zero crossing rate, and spectral entropy and power spectrum frequency-domain features could be extracted.

#### 2.5.1. Power Spectrum

The power spectrum represents the variation of the acoustic as a function of frequencies, and we applied the Welch power spectrum estimation method to conduct the feature analysis. Welch's method [20] is more traditional than the direct power spectrum methods and computationally less expensive and robust [21]. The latter are used with too large or small information data without spectral line fluctuations and poor resolution conditions.

Given a discrete acoustic feeding signal $X_N(n)$, the signal is divided into L segments, and each segment is M in length. Each segment can overlap with each other, and assuming that the overlap ratio between each segment is 50%, the number of segments is

$$L = \frac{(N - M/2)}{M - 2}. \tag{1}$$

The data in the $i$-th are noted as

$$x_N^i = \left[ n + \frac{(i-1)M}{2} \right]. \tag{2}$$

Figure 2 shows the process the fast Fourier transform. Windows $w(n)$ were added to each segment, and Fourier transform (FT) was performed; the windowed FFT is expressed as

$$X_i\left(e^{jw}\right) = \sum_{n=0}^{M-1} x_i(n) w(n) e^{-jw}. \tag{3}$$

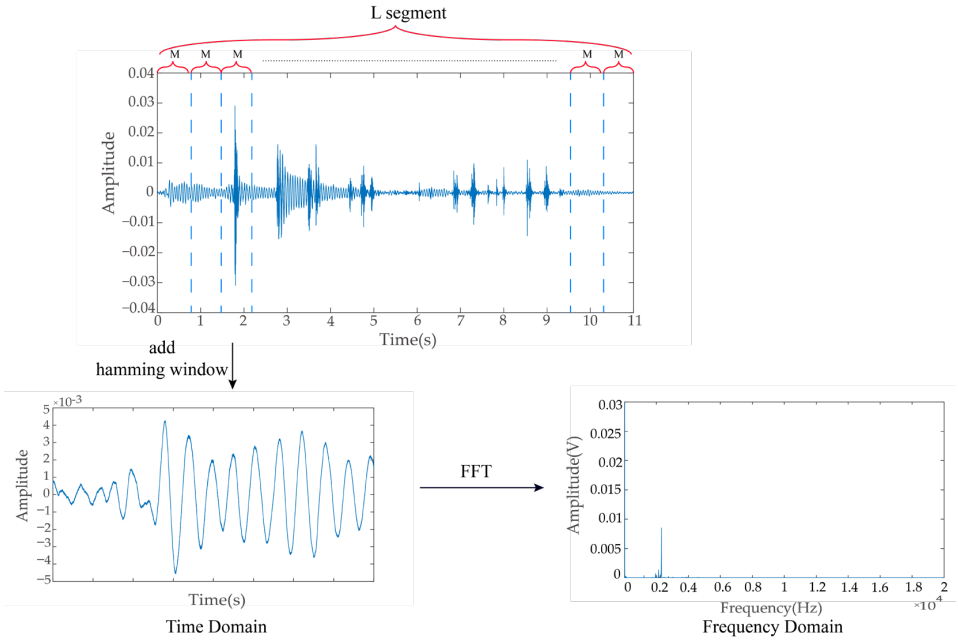



**Figure 2.** Schematic diagram of the fast Fourier transform of ingestion acoustic signal.

The power spectrum of each segment $I_i\left(e^{jw}\right)$ may be expressed as

$$I_i\left(e^{jw}\right) = \frac{1}{MU}\left|X_i\left(e^{jw}\right)\right|^2, \tag{4}$$

where U is the normalization factor.

The formula of the power spectrum $\hat{S}_x(e^{jw})$ after averaging may be expressed as

$$\hat{S}_x\left(e^{jw}\right) = \frac{1}{L}\sum_{n=0}^{M=1}\frac{1}{MU}\left|X_i\left(e^{jw}\right)\right|^2. \quad (5)$$

2.5.2. Short-Time Zero-Crossing Rate

The symbolic vocal change in the discrete signal amplitude is called the zero crossing, and the number of trans-zeros per unit time is called the average number of zero crossings. The signal energy frequency during the largemouth bass feeding was lower than the background noise energy frequency; thus, this feature could be used as an acoustic characteristic of the group of fish. $Z_n$ indicates the short-time zero-crossing rate of the largemouth black bass sound signal $x_n(m)$

$$Z_n = \frac{1}{2}\sum_{M=0}^{N-1}|\mathrm{sgn}[x_n(m)] - \mathrm{sgn}[x_n(m-1)]|, \quad (6)$$

where sgn [] is the sign function:

$$\mathrm{sgn}[x] = \begin{cases} 1, & (x \geq 0) \\ -1, & (x < 0) \end{cases}. \quad (7)$$

2.5.3. Short-Time Average Amplitude

The complexity of the acoustic signal analysis stems from the fact that the fish feeding signal is a random non-smooth signal; hence, we analyzed the change in its amplitude from the time-domain perspective. Additionally, the short-time average energy was too sensitive to the high level; thus, we used the short-time average amplitude instead. We obtained the $n$-th frame of the acoustic signal by dividing the time-domain signal of the largemouth bass acoustic shape into frames and adding the window function; then, the following equations were satisfied:

$$x_n(m) = w(m)x(n+m) \qquad 0 \leq m \leq N-1, \quad (8)$$

$$w(m) = \begin{cases} 1, m = 0 \sim (N-1) \\ 0, m = \text{other values} \end{cases}, \quad (9)$$

where $n$ = 0, $T$, 2$T$, . . . , $N$ is the frame length, and $T$ is the frame shift length. Let the short-time average amplitude of the n-th frame of the sound signal be expressed by $N$; then, the short-time average amplitude of the largemouth bass feeding sound is calculated as

$$M_n = \sum_{m=0}^{N-1}|x_n(m)|. \quad (10)$$

2.5.4. Spectral Entropy

Spectral entropy is a popular and simple method derived from Shannon's information entropy to perform narrow-band signal detection, and it has demonstrated success in speech and animal vocalization detection [22]. The time-domain signal can be converted to a frequency-domain signal using Fourier transformation, and the frequency-domain parameters have higher noise immunity than the time-domain parameters. The spectral entropy, as a kind of signal frequency-domain feature, indicates the information order degree [23]. The spectral entropy is not affected by the signal size but is only related to the signal-to-noise ratio, which is expressed by the FFT, where the subscript n indicates the $n$-th frame, and k indicates the $k$-th spectral line. The short-time energy in the frequency domain is

$$E_n = \sum_{k=0}^{N/2} X_n(\mathrm{k})X_n^*(k). \quad (11)$$

The normalized spectral probability density function for each frequency component is defined as

$$p_n(k) = \frac{Y_n(\mathrm{k})}{\sum_{I=0}^{N/2} Y_n(l)} = \frac{Y_n(\mathrm{k})}{E_n}. \quad (12)$$

The short-time spectral entropy of the largemouth bass feeding signal frames is calculated as

$$H_n = -\sum_{I=0}^{\frac{N}{2}} P_n(k) \ln(p_n(k)). \quad (13)$$

### *2.6. Statistical Analysis*

To determine the change pattern of each characteristic parameter with the acoustic signal of the largemouth bass feeding, we used SPSS STASTIC 22 to conduct the statistical analyses. We mainly used a one-way ANOVA linear analysis to analyze the main power value of the power spectrum and culture density, the Pearson correlation coefficient to analyze the correlation between the short-time mean amplitude and culture density, and the LSD method to conduct a one-way multiple comparison significance analysis to compare the differences between the groups.

## 3. Results

### *3.1. Power Spectrum*

Figure 3 shows the power spectra of the largemouth bass feeding at different culture densities. After analyzing the power spectrum of multiple groups, we found that the power spectrum of the background noise ranged from −160 to −120 dB, the frequency range of the largemouth bass feeding sound signal was 1–20 kHz, and the power ranged from −160 to −55 dB, but its larger energy was generally concentrated at 1.2–5.4 kHz (see dotted box in Figure 1). The higher power value of the group with more tails can be seen in the image.

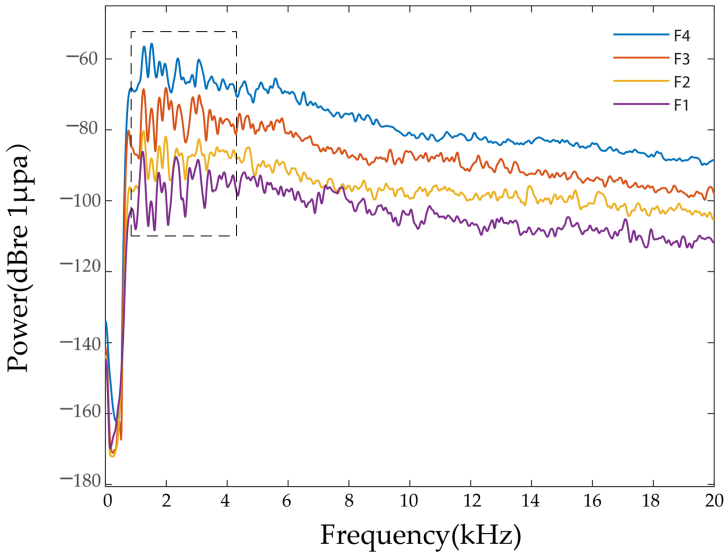



**Figure 3.** Comparison of feeding acoustic power spectrum of largemouth bass under different breeding densities.

We randomly selected 20 feeding sound signals in each group of largemouth bass for the power spectrum analysis, and we extracted the typical power spectrum parameters, including the feeding sound vocalization frequency range of the largemouth bass and the main peak frequency found with the power spectrum and statistical analysis. Table 2 shows the statistical characteristics of the power spectra of the largemouth bass with different culture densities.

**Table 2.** Statistical characteristic values of power spectrum of largemouth bass at different culture densities.

| Group | Breeding Density (Fish·m$^{-3}$) | Frequency Range of Feeding Vocalizations (kHz) | Power Spectrum Main Peak Frequency (kHz) | Main Power Value (dBre 1 μPa) |
|---|---|---|---|---|
| F1 | 4 | 1–20 | 2.21 ± 1.31 $^{a}$ | −72.61 ± 3.34 $^{d}$ |
| F2 | 8 | 1–20 | 1.96 ± 0.99 $^{a}$ | −66.54 ± 3.69 $^{c}$ |
| F3 | 12 | 1–20 | 1.72 ± 0.56 $^{a}$ | −63.81 ± 2.89 $^{b}$ |
| F4 | 16 | 1–20 | 1.76 ± 0.58 $^{a}$ | −59.07 ± 1.89 $^{a}$ |

Note: values with different letters within the same column indicate significant difference ($p < 0.05$).

As shown in Table 2, the main feeding sound frequencies and the distinguishable spectral range of the background noise of the largemouth bass at different culture densities ranged from 1 to 20 kHz. The results of a statistical analysis on the characteristics of the feeding sound signals of the largemouth bass at different culture densities in the distinguishable frequency range revealed that the main peak power of the power spectra of different culture densities was significantly different ($p < 0.05$), whereas the differences in the main peak frequencies of the power spectra were not significant ($p > 0.05$). The main peak frequencies mainly appeared in the range of 1.2–3.0 kHz; therefore, when conducting the frequency domain analysis, the power value can be used as a quantitative parameter to measure different breeding densities. We performed a regression analysis on the different breeding densities and main power values and found that with the increase in breeding densities, the main power value of the feeding acoustic signal also increased, and the main power value (y) in the frequency range of 1–20 kHz and the breeding density (N) showed a linear relationship, $y = 2.140 \log_{10}(N) - 8.577$, $R^2 = 0.7160$ (>0.7), indicating an accurate linear fit.

### *3.2. Short-Time Zero Crossing Rate*

Figure 4 shows the results of quantifying the feeding behavior of the fish under different culture conditions based on the short-time average zero-crossing rate. As can be seen in Figure 3, certain fluctuations in the short-time average zero-crossing rate of the fish in different culture densities were maintained when they were not feeding, and, after the fish started feeding, the zero-crossing rate rapidly dropped from the mean value of 1500 to the mean value of 500 in the nonfeeding state, which was maintained for a period of time. After this, the zero-crossing rate rose to the mean value of 1000, at which time the fish finished swallowing, started chewing the feed, and finished the feeding process. At this time, the mean value of the zero-crossing rate fluctuated from 500 to 1000. The feeding sound belonged to the low-frequency signal, and the zero-crossing rate of the low-frequency signal was low, whereas the zero-crossing rate of the background noise was relatively high. Because the difference between the zero-crossing rate of the swallowing and chewing parts was not too obvious, identifying the two sounds with the short-time average zero-crossing rate was not possible, but the short-time average zero-crossing rate could reflect the change in the largemouth bass feeding behavior.

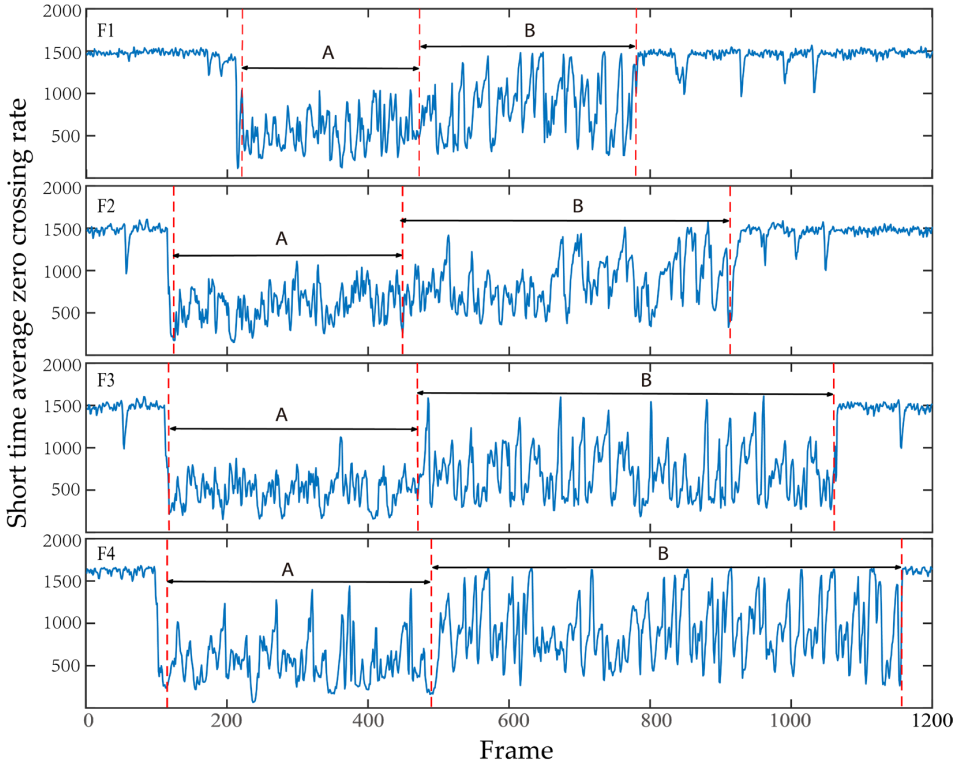



**Figure 4.** Short-term average zero crossing rate of feeding acoustic signal of largemouth bass with different breeding densities (A is the ingestion stage; B is the chewing stage): F1 represents the experimental group of breeding density of 4; F2 represents the experimental group of breeding density of 8; F3 represents the experimental group of breeding density of 12; F4 represents the experimental group of breeding density of 16.

### *3.3. Short-Time Average Amplitude*

We randomly selected one feeding signal from each culture density group, and Figure 4 shows the quantification results of the feeding behavior of the largemouth bass at different culture densities based on the short-time average amplitude. The short-time average amplitude can visually reflect the change in energy, which can be used to judge the occurrence of feeding behavior of largemouth bass. The difference in the short-time average amplitude of the swallowing sound compared with the chewing sound was more obvious in one feeding process. The short-time average amplitude of the feeding sound of the largemouth bass greatly varied with the different culture densities, and Figure 5 shows that the time of swallowing, chewing, and the whole feeding process of the largemouth bass increased with the increase in culture density. Therefore, the short-time average amplitude can be used as an acoustic feature to distinguish the swallowing and chewing sound signals from the background noise.

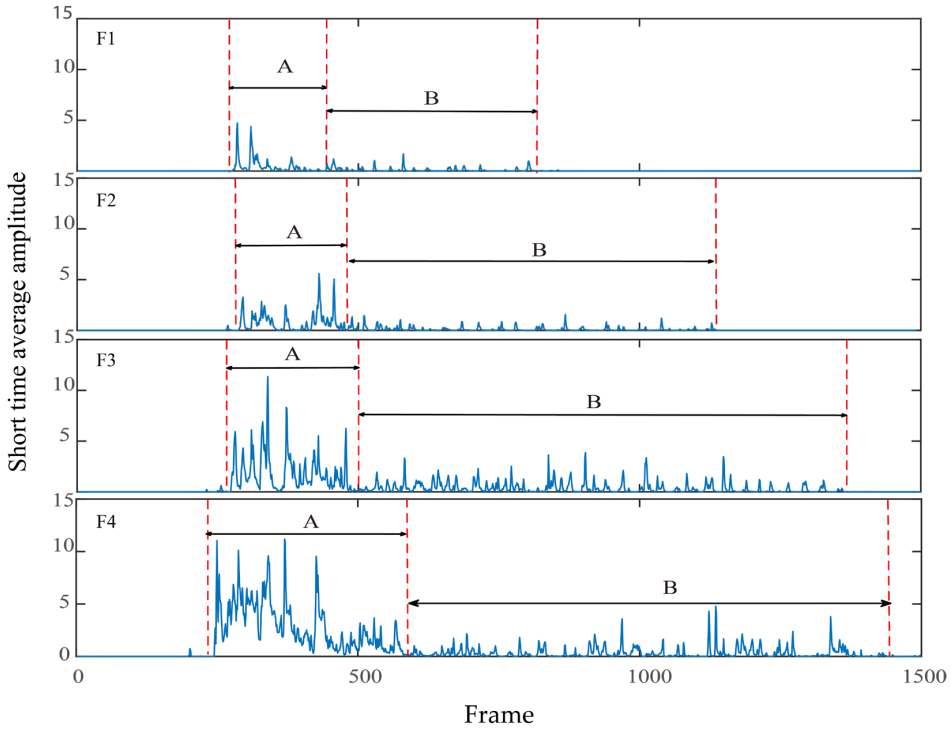



**Figure 5.** Short-time average amplitude of largemouth bass feeding call (A is the ingestion stage; B is the chewing stage): F1 represents the experimental group of breeding density of 4; F2 represents the experimental group of breeding density of 8; F3 represents the experimental group of breeding density of 12; F4 represents the experimental group of breeding density of 16.

We randomly selected the short-time average amplitude of each group of 10 feeding audio signals to extract the short-time average amplitude of the swallowing and chewing process, and then the average value was obtained to compare the correlation between the short-time average amplitude and the breeding density. It is obvious from Table 3 that the correlation coefficient of the short-time average amplitude of the signal of largemouth bass swallowing and the number of fish reached 0.880, whereas the correlation coefficient of the chewing sound signal and the number of fish was only 0.487. Moreover, the positive correlation coefficient of the swallowing sound and number of fish was generally in the range of 0.5 to 1, which means that the correlation was stronger, and the correlation coefficient of the chewing sound signal and the number of fish was in the range of 0 to 0.5, which means that the correlation was weaker. Thus, the correlation between the swallowing sound and number of fish was stronger and superior to that between the chewing sound and the number of fish.

**Table 3.** Correlation analysis between short-term mean amplitude of feeding sound and breeding density of largemouth bass ($p < 0.05$).

| Group | Breeding Density (Fish·m$^{-3}$) | Acoustic Signal | |
|---|---|---|---|
| | | Swallowing | Chewing |
| F1 | 4 | $0.18 \pm 0.06^{d}$ | $0.07 \pm 0.03^{b}$ |
| F2 | 8 | $0.43 \pm 0.23^{c}$ | $0.17 \pm 0.08^{a}$ |
| F3 | 12 | $0.80 \pm 0.17^{b}$ | $0.14 \pm 0.05^{a}$ |
| F4 | 16 | $2.50 \pm 0.31^{a}$ | $0.16 \pm 0.11^{a}$ |
| Correlation coefficient | | 0.880 | 0.487 |

Note: values with different letters within the same column indicate significant difference ($p < 0.05$).

### *3.4. Spectral Entropy*

Figure 6 shows the results of quantifying the feeding behavior of the fish under different cultures based on the signal spectral entropy. A more obvious difference existed between the feeding sound and noise at the beginning of the largemouth bass feeding. The spectral entropy value of the noise segment before feeding was maintained at about 8, and the entropy value essentially fluctuated above and below 5 during the feeding period. Moreover, the amplitude of the signal of largemouth bass in the feeding stage was essentially the same, fluctuating between 4 and 6, and it was different from the environmental noise. These results indicate that spectral entropy value can represent the differentiation of the largemouth bass feeding process and can be used to identify the feeding signal.

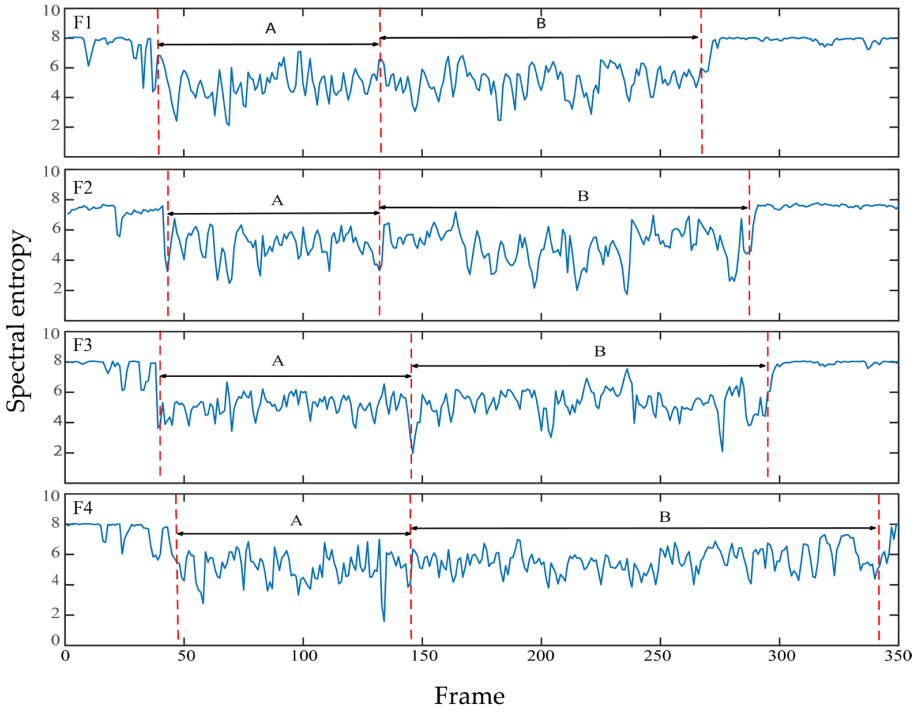
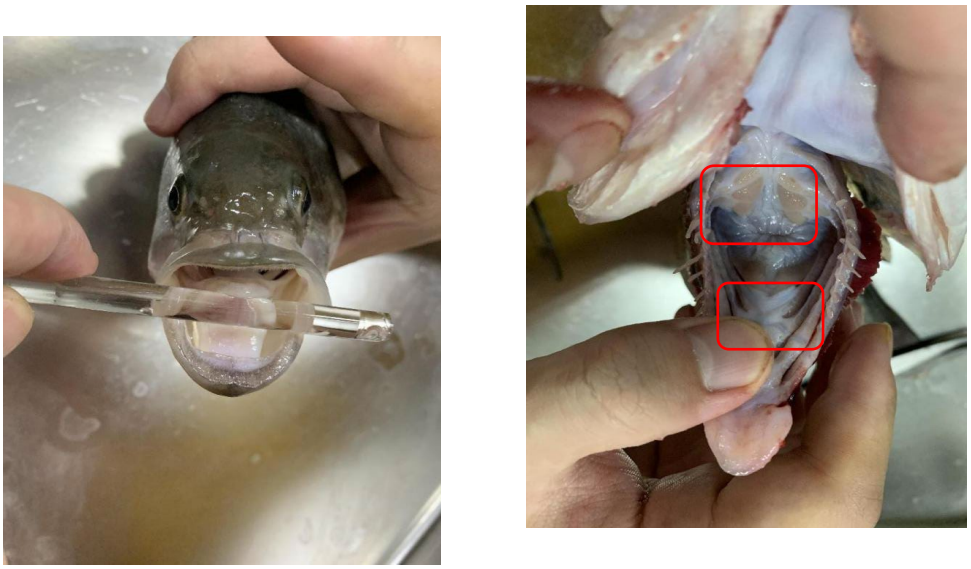



**Figure 6.** Spectrum entropy of largemouth bass feeding signal under different breeding densities (A is the ingestion stage; B is the chewing stage): F1 represents the experimental group of breeding density of 4; F2 represents the experimental group of breeding density of 8; F3 represents the experimental group of breeding density of 12; F4 represents the experimental group of breeding density of 16.

## 4. Discussion

Conducting acoustic studies on aquatic organisms is difficult because of the complexity of the water environment and because fish do not have vocal cords; thus, their vocal mechanisms are different from those of terrestrial animals. Largemouth bass produce many feeding acoustic signals after feeding, and, according to the vocal mechanism, most of them are passive vocalizations. Scholars who conducted studies on the vocal mechanisms of fish found that eight main types of fish vocalizations exist: drumming, cavitation, hydrodynamic, aeration, percussion, string, respiration, and friction mechanisms [24]. Largemouth bass mainly use their upper and lower jaws and pharyngeal teeth to produce their feeding sounds [25]. Figure 7 highlights the swallowing and chewing organs in red. According to the characteristics of the largemouth bass swallowing sound signal, the cavitation mechanism is more consistent with the swallowing sound vocal characteristics; when the upper and lower jaws of the largemouth bass open, the gill cover will be tightly closed, causing the inner pressure of the mouth to be lower than the outer pressure, which causes the feed to be sucked into the mouth due to the pressure difference. The chewing sound is mainly caused by the grinding of feed in the mouth by pharyngobranchial teeth

and pharyngeal teeth, accompanied by the expulsion of broken feed from the gill. Therefore, the masticatory sound is regulated by a friction mechanism and cavitation mechanism [26].



(**a**) (**b**)

**Figure 7.** Swallowing vocal parts (**a**): Premaxillary tooth and chewing vocal parts (**b**): Upper red frame: pharyngobranchial teeth and bottom red frame: pharyngeal teeth.

The feeding signal frequencies of the largemouth bass at different culture densities all ranged from 1 to 20 kHz; thus, the feeding sound frequencies may not have been related to the culture density and may have only been related to the fish species, which is consistent with the experimental findings obtained by Ren et al. [27] using rhododendron. Lagardère et al. [28] extracted feeding signal frequencies for turbot experiments that were essentially consistent with our findings, whereas Qu et al. [18] and Cao et al. [19] found that the frequency range of the feeding acoustic signals was 1–10 kHz, which is slightly different from our results. The former used the frequency range of feeding sound of largemouth bass based on resonance peak analysis, while the present experiment uses power spectrum analysis to find the distinguishable noise range of 1–20 kHz; the latter selected larger fish sizes than the present experiment. Hence, it is conjectured that the frequency range of feeding sound may be inversely proportional to the size of the fish. This was probably because the authors of both experiments did not analyze the background noise and high-frequency band signals. However, Qu et al. found the same locations of spectral peaks as us. Additionally, they found that the highest energy feeding vocal range of turbot and rainbow trout was 7–9 kHz and 4–6 kHz [15], and the reason for this difference may be due to the different vocal mechanisms of various fish. The main peak value obtained from the power spectrum increased with an increasing culture density, which Qu et al. also found [18], but their main power value was considerably higher than ours, and the reason for this difference was the difference in culture density. Moreover, in addition to other scholars, we demonstrated a positive correlation existed between the main peak value of the power spectrum and the culture density [17,18]; therefore, this could provide information about the density of the fish population density.

Mallekh et al. [16] suggested the potential role of the acoustic characteristics of fish feeding in controlling feed allocation in aquacultures. As we demonstrated, the short-time mean amplitude, short-time mean zero-crossing rate, and spectral entropy can be used as acoustic parameters to identify the largemouth bass feeding process [29,30]. The mean amplitude of the largemouth bass rearing short time differed significantly among the

different experimental groups, which was mainly caused by the different breeding densities of the fish. In addition, the amplitude of the swallowing sound signal was considerably higher than that of the chewing sound signal, which, as demonstrated by the results of existing studies [31], was due to the different transmission media of the two types of sounds in the largemouth bass. In the experimental group of largemouth bass with different breeding densities, the short-time mean zero-crossing in the swallowing phase was about 500, and, in the chewing phase, it was about 1000; both showed a consistent trend over time. Additionally, a dolphin's zero-crossing rate was also stable at a fixed value at the time of whistling [32]; thus, the short-time mean zero-crossing rate was species-dependent. In addition, the spectral entropy values of the feeding sounds at different breeding densities were consistent. If we can rely on features such as the short-time average amplitude, zero-crossing rate, and spectral entropy to establish the identification model of the feeding sounds of largemouth bass, we can effectively save costs, and this can also provide a strong research basis for the classification of hunger level based on feeding sounds later [33–35]. We were unable to determine the effect of feed particle size on the feeding signal, and whether a high culture density would also block and attenuate the signal transmission in practice. To use the feeding vocal signal for automatic feeding in aquacultures, the characteristics of the vocal signal of largemouth bass at different growth stages and the effect of different sizes of pellets on the feeding sound of largemouth bass need to be considered in the future.

## 5. Conclusions

We successfully found that the short-time average amplitude of feeding signal can be distinguished from the background noise in the time-domain characteristics. The swallowing and chewing sounds are positively correlated with culture density, and the swallowing sound correlation is better. The average zero crossing of largemouth bass in different breeding densities suddenly decreased to about 500 during the swallowing stage, and increased to about 1000 during the chewing stage. The two can be used as the characteristic parameters of automatic signal recognition of largemouth bass during feeding. The spectral entropy amplitude of largemouth bass in feeding stage of different breeding densities was maintained at about 4–6. In the power spectrum, the main frequency spectrum of feeding sound and background noise of cultured density largemouth bass were both in the range of 1–20 kHz, and the main peak frequency of feeding sound was in the range of 1.2–5.4 kHz. The main power value of the power spectrum was positively correlated with the culture density and the linear relationship was $y = 2.140 \log_{10}(N) - 8.577$, $R^2 = 0.7160$.

**Author Contributions:** Conceptualization, H.L. and S.L.; data curation, R.Q.; formal analysis, R.Q.; funding acquisition, H.L.; methodology, H.L. and S.L.; project administration, H.L. and S.L.; resources, R.Q.; software, R.Q.; writing—original draft, R.Q.; writing—review and editing, R.Q. All authors have read and agreed to the published version of the manuscript.

**Funding:** This work was supported by the National Key R&D Program of China: 2021YFE0108700.

**Institutional Review Board Statement:** This experiment complied with the regulations and guidelines established by the Animal Care and Use Committee of Fishery Machinery and Instrument Research Institute, Chinese Academy of Fishery Sciences (FMIRI-AWE-2022-001, approved on 30 September 2022).

**Informed Consent Statement:** Not applicable.

**Data Availability Statement:** Not applicable.

**Acknowledgments:** The authors would like to express their thanks to H.L. of the Fishery Machinery and Instrument Research Institute, Chinsese Academy of Fishery Sciences for polishing this article. The authors are thankful for the financially support from the National Key R&D Program of China (2021YFE0108700).

**Conflicts of Interest:** The authors declare no conflict of interest.

## References


1. Wu, Y.; Wang, X.; Zhang, X.; Shi, Y.; Li, W. Locomotor posture and swimming-intensity quantification in starvation-stress behavior detection of individual fish. *Comput. Electron. Agric.* **2022**, *202*, 107399. [CrossRef]
2. Zeng, Y.; Yang, X.; Pan, L.; Zhu, W.; Wang, D.; Zhao, Z.; Liu, J.; Sun, C.; Zhou, C. Fish school feeding behavior quantification using acoustic signal and improved Swin Transformer. *Comput. Electron. Agric.* **2023**, *204*, 107580. [CrossRef]
3. Zhaohui, Z.; Yuan, P. Study on the characteristics of dolphins click signal. In Proceedings of the 2020 5th International Conference on Communication, Image and Signal Processing (CCISP), Chengdu, China, 13–15 November 2020.
4. Zhou, Y.L.; Xu, X.M.; Zhang, X.H.; Huang, L.F.; Xiao, F.G.; He, Y.W. Vocalization behavior differs across reproductive stages in cultured large yellow croaker *Larimichthys crocea* (*Perciformes: Sciaenidae*). *Aquaculture* **2022**, *556*, 738267. [CrossRef]
5. Ladich, F. Sound Production and acoustic communication. In *The Senses of Fish. Adaptations for the Reception of Natural Stimuli*; Springer: Berlin/Heidelberg, Germany, 2004; pp. 210–230.
6. Lindseth, A.; Lobel, P.S. Underwater Soundscape Monitoring and Fish Bioacoustics: A Review. *Fishes* **2018**, *3*, 36. [CrossRef]
7. Fengdeng, Z. *Study on Adaptive System Based on Feedback of Feeding Behavior of Micropterus salmoides in Recirculating Aquaculture System*; Zhejiang University: Hangzhou, China, 2019.
8. Michaelis, P.; Thierry, B. A comparative study of automatic feeding and automatic feeding and self-feeding in juvenile Atlantic salmon (*Salmo salar*) fed diets of different energy levels. *Aquaculture* **1996**, *145*, 245–257.
9. Li, D.L.; Liu, C. Recent Advances and Future Outlook for Artificial Intelligence in Aquaculture. *Smart Aquac.* **2020**, *2*, 1–20.
10. Le, Z.Y. Exploration and suggestions for effective protection of offshore fishery resources based on acoustic technology. *China Aquac.* **2022**, *5*, 58–60.
11. Smith, D.V.; Tabrett, S. The use of passive acoustics to measure feed consumption by *Penaeus monodon* (giant tiger prawn) in cultured systems. *Aquac. Eng.* **2013**, *57*, 38–47. [CrossRef]
12. Christopher, L. The Use of Feeding Noises to Determine the Algal Foods Being Consumed by Individual Intertidal Molluscs. *Oecologia* **1979**, *40*, 1–17.
13. Li, D.; Wang, Z.; Wu, S.; Miao, Z.; Du, L.; Duan, Y. Automatic recognition methods of fish feeding behavior in aquaculture: A review. *Aquaculture* **2020**, *528*, 735508. [CrossRef]
14. Cao, Z.L.; Shen, M.T.; Li, Z.C.; Wang, Z.H.; Wang, X.X. Characteristics of feeding acoustic of *Litopenaeus vannamei* fed with pellets of different sizes. *South China Fish.* **2022**, *19*, 26–33.
15. Lagardère, J.P.; Mallekh, R.; Mariani, A. Acoustic characteristics of two feeding modes used by brown trout (*Salmo trutta*), rainbow trout (*Oncorhynchus mykiss*) and turbot (*Scophthalmus maximus*). *Aquaculture* **2004**, *240*, 607–616. [CrossRef]
16. Mallekh, R.; Lagardère, J.P.; Eneau, J.P.; Cloutour, C. An acoustic detector of turbot feeding activity. *Aquaculture* **2003**, *221*, 481–489. [CrossRef]
17. Tang, T.L.; Tang, R.; Liu, S.J.; Chen, J.; Miao, L.; Zhou, R. Acoustic control of feeding in Tilapia culture. *Prog. Fish. Sci.* **2014**, *35*, 40–43.
18. Qu, R.; Liu, H.; Liu, J.W.; Zhang, Y.L. Acoustic signal characteristics of Largemouth bass (*Micropterus salmoides*) in feeding process and the effects of breeding density. *Fish. Mod.* **2021**, *48*, 55–63.
19. Cao, X.H.; Liu, H.; Qi, R.Y.; Zhang, C.L.; Liu, S.J. Acoustic characteristics of the feeding pellets for *Micropterus salmoides* in circulating aquaculture. *Trans. Chin. Soc. Agric. Eng.* **2021**, *37*, 219–225.
20. Li, X.Y.; Guan, Y.H.; Luo, M.X.; Wu, B.Y. Modal parameter identification of covariance-based stochastic subspace identification based on Welch method. *Chin. J. Theor. Appl. Mech.* **2022**, *54*, 2850–2860.
21. Farheen, S.; Awwab, M.; Sameena, N. Deep neural network for EEG signal-based subject-independent imaginary mental task classification. *J. Ichthyol.* **2008**, *48*, 640.
22. Marco, R.; Daniel, J.; Johan, P. Soft-output signal detection for cetacean vocalizations using spectral entropy, K-means clustering and the continuous wavelet transform. *Ecol. Inform.* **2023**, *74*, 101990. [CrossRef]
23. Yubiry, G.; Ronaldo, P. Similarity of muscial timbres using FFT-acoustic descriptor analysis and machine learning. *Eng* **2023**, *4*, 555–568.
24. Kasumyan, A.O. Sounds and sound production in fishes. *J. Ichthyol.* **2008**, *48*, 981–1030. [CrossRef]
25. Yu, Y.J.; Wu, Y.F. Comparative Studies of the Oral-Cavity Teeth of Several Perciform Fishes. *J. Ocean. Univ. China* **2004**, *34*, 29–36.
26. Scholz, K.; Ladich, F. Sound production, hearing and possible interception under ambientnoise conditions in the topmouth minnow Pseudorasbora parva. *J. Fish Biol.* **2006**, *69*, 892–906. [CrossRef]
27. Ren, X.M.; Gao, D.Z.; Yao, Y.l.; Yang, F.; Liu, J.F.; Xie, F.J. Study on the vocalization and signal characteristics of rhododendron. *J. Dalian Fish. Univ.* **2007**, *22*, 124–128.
28. Lagardere, J.P.; Mallekh, R. Feeding sounds of turbot (*Scophthalmus maximus*) and their potential use in the control of food supply in aquaculture. *Aquaculture* **2000**, *189*, 251–258. [CrossRef]
29. Liu, C. An improved speech endpointed detection algorithm analyses based on short-time average amplitude. *J. Northwest Univ. Natl. (Nat. Sci.)* **2009**, *30*, 56–59.
30. Liu, B.; Hao, X.H.; Cai, X. Classification method of radio fuze target and interference signal based on power spectrum entropy. *J. Beijing Univ. Aeronaut. Astronaut.* **2022**, *48*, 1–10. [CrossRef]
31. Ladich, F.; Anderw, H. Sonic/Vocal-Acousticolateralis Pathways in Teleost Fishes: A Transneuronal Biocytin Study in Mochokid Catfish. *J. Comp. Neurol.* **1996**, *374*, 493–505. [CrossRef]

32. Yang, L.H.; He, D.Y.; Fang, L.; He, L.G. The Detection Method of Dolphin Vocal Endpoint Based on Time-Frequency Characteristics. *J. Appl. Acoust.* **2022**, *13*, 1–10. Available online: http://kns.cnki.net/kcms/detail/11.2121.o4.20220811.1518.004.html (accessed on 12 August 2022).
33. Li, L.; Tu, Q.Z.; Huang, H.Y.; Zhao, S.M.; Xiong, S.B.; Ma, Z.Y. Freshwater Fish Identification Based on Passive Underwater Acoustic Signals. *Trans. Chin. Soc. Agric. Mach.* **2017**, *48*, 166–171.
34. Huang, H.Y.; Yang, Y.W.; Li, L.; Zhao, S.M.; Xiong, S.B.; Tu, Q.Z. Mixed Proportion Identification of Freshwater Fish Based on Passive Underwater Acoustic Signals. *Trans. Chin. Soc. Agric. Mach.* **2019**, *50*, 215–221.
35. Yang, Y.W.; Huang, H.Y.; Feng, W.X.; Li, L.; Xiong, S.B.; Zhao, S.M. Mixed quantities prediction of freshwater fish based on passive underwater acoustic signals. *Trans. Chin. Soc. Agric. Mach.* **2020**, *39*, 147–152.

**Disclaimer/Publisher's Note:** The statements, opinions and data contained in all publications are solely those of the individual author(s) and contributor(s) and not of MDPI and/or the editor(s). MDPI and/or the editor(s) disclaim responsibility for any injury to people or property resulting from any ideas, methods, instructions or products referred to in the content.